

Binding of Phthalate Plasticizers to Human Serum Albumin in Vitro: A Multispectroscopic Approach and Molecular Modeling

Xi-Min Zhou,^{†,‡} Wen-Juan Lü,^{†,‡} Li Su,^{†,‡} Zhi-Jie Shan,^{†,‡} and Xing-Guo Chen^{*,†,‡,§}

[†]State Key Laboratory of Applied Organic Chemistry and [‡]Department of Chemistry, Lanzhou University, Lanzhou 730000, China

[§]Key Laboratory of Nonferrous Metal Chemistry and Resources Utilization of Gansu Province, Lanzhou 730000, China

ABSTRACT: As endocrine-disrupting chemicals, a few frequently used phthalate plasticizers were banned or restricted for use as additives in food in some countries. The interaction mechanisms between three phthalate plasticizers with human serum albumin (HSA) were studied by fluorescence (quenching, synchronous, and three-dimensional), UV–vis absorption, circular dichroism (CD), and Fourier transform infrared (FT-IR) spectroscopy, in combination with molecular modeling under simulative physiological conditions, respectively. The results obtained from fluorescence quenching data revealed that the plasticizers–HSA interaction altered the conformational structure of HSA. Meanwhile, the alterations of HSA secondary structure in the presence of phthalate plasticizers were investigated. The binding distances for the plasticizers–HSA system were provided by the efficiency of fluorescence resonance energy transfer. Furthermore, the thermodynamic analysis implied that hydrophobic forces were the main interaction for the plasticizers–HSA system, which agreed well with the results from the molecular modeling study.

KEYWORDS: phthalate plasticizers, human serum albumin (HSA), fluorescence quenching, circular dichroism (CD), Fourier transform infrared (FT-IR)

INTRODUCTION

Food safety remains a public concern all over the world. In the past, phthalate esters were widely used as plasticizers in industrial processes, to impart flexibility and resiliencing to plastic products,¹ but not as plasticizers in consumer products,^{2,3} because this class of substances can mimic, block, or interfere with hormones in the body and easily affect development and reproduction of human.⁴ However, recently in Taiwan some phthalate plasticizers were added to a few nutritional supplements, vitamins, foods, and beverages as an alternative for palm oil in an effort to cut costs. Several phthalate plasticizers, such as diethyl phthalate (DEP), dibutyl phosphate (DBP), diisobutyl phthalate (DIBP), diethylhexyl phthalate (DEHP), and butyl benzyl phthalate (BBP) are classified as toxic materials due to their reproductive toxicity,⁵ and they have been banned or restricted in toys and some other plastic products in the European Union, United States, Australia, etc. and will be banned or limited in more countries in the near future.⁴ Phthalate plasticizers can lead to environmental pollution and be directly uptaken by animals via food or air and potential bioaccumulation and transfer through the food chain⁶ and cause harm to health of human finally. It is reported that the phthalate plasticizers are possibly related to asthma and airway diseases in children.⁷ In this paper, DEP, DBP, and DIBP (structures shown in Figure 1) served as typical model compound to construct the study method of the interaction mechanism of phthalate plasticizers and human serum albumin (HSA).

Among biomacromolecules, HSA is the most crucial carrier protein in blood plasma, accounting for approximate 60% of the total protein, corresponding to a concentration of 42 g/L,⁸ which has many important physiological and pharmacological functions.⁹ From the three-dimensional structure of HSA, it can

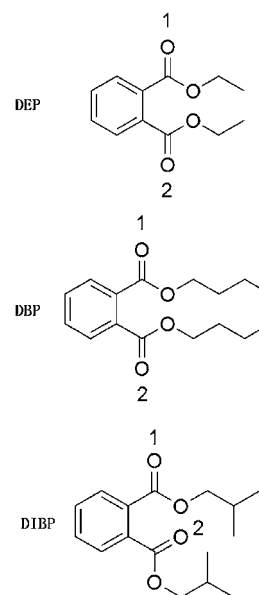


Figure 1. The chemical structures of DEP, DBP, and DIBP.

be seen that HSA is a single polypeptide chain of 585 amino acids containing α -helical portions, and it forms from three homologous domains (I–III) that assemble to form a heart-shaped molecule. Each domain can be segmented into two subdomains (A and B), which consist of six and four α -helices, respectively. HSA is the major soluble protein constituents of

Received: October 26, 2011

Accepted: December 29, 2011

Published: December 29, 2011

the circulatory system and plays the major role in the transport and deposition of a large number of small molecules, and some works on the interaction between small molecules with HSA have been carried out.^{2,10,11} Consequently, the interaction between ligands and HSA has already become an important research field in chemistry, life sciences, nutriology, clinical medicine, and toxicology. So the investigation of the interaction between phthalate plasticizers and HSA is significant, which can imply some theoretical foundation potentially for the harm to the human body from phthalate plasticizers.

In the present work, the interactions of three phthalate plasticizers (DEP, DBP and DIBP) with HSA were investigated in vitro under simulative physiological conditions (pH 7.4, ionic strength 0.1) using a multispectroscopic approach consisting of fluorescence quenching spectroscopy, UV-vis absorption spectroscopy, CD spectroscopy, FT-IR spectroscopy, three-dimensional fluorescence spectroscopy, and molecular modeling method for the first time, and the result of each method was compatible and complemented one another. The study indicated that the intrinsic fluorescence of HSA was quenched through static quenching mechanism for the plasticizers-HSA system. Fluorescence quenching technology showed that the interaction between three ligands and HSA induced a change of microenvironment of a Trp residue in HSA. The conformational changes of HSA were further proved by the UV-vis absorption, CD, FT-IR and three-dimensional fluorescence spectroscopy data quantitatively and qualitatively. The identification of binding sites and the molecular modeling method showed that the binding sites were located at site I of HSA for three ligands, and they were bound to HSA through the hydrophobic forces and hydrogen bonds. In conclusion, the three phthalate plasticizers have the same main functional group and are phthalate esters, so the interaction mechanism between three ligands and HSA were analogous.

MATERIALS AND METHODS

Materials. HSA was purchased from Sigma Chemical Co. and was used without further purification; the molecular weight of HSA was assumed to be 66 500 to calculate the molar concentrations. All HSA solutions were prepared in pH 7.40 buffer solution, and HSA stock solution (3.0×10^{-5} mol/L) was kept in the dark at 277 K. Tris (0.2 mol/L)-HCl (0.1 mol/L) buffer solution containing NaCl (0.1 mol/L) was used to keep the pH of the solution at 7.40. NaCl (1.0 mol/L) solution was used to maintain the ionic strength at 0.1. Dilutions of the HSA stock solution in Tris-HCl buffer were prepared immediately before use. DEP, DBP, DIBP, phenylbutazon (PB), flufenamic acid (FA), and digitoxin (Dig) were of analytical grade, and purchased from J&K Scientific Ltd. (Beijing, China). The stock solutions of 5.0×10^{-3} M DEP, 1.0×10^{-3} M DBP, and 1.0×10^{-3} M DIBP were prepared in anhydrous methanol, and 1.0×10^{-3} M PB, 1.0×10^{-3} M FA, and 1.0×10^{-3} M Dig were prepared in anhydrous ethanol. All other reagents were of analytical reagent grade, and double distilled water was used throughout the experiments.

Fluorescence Spectroscopy. All the fluorescence spectra were recorded on a RF-5301PC spectrofluorophotometer (Shimadzu) at 298 K, using 5 nm/5 nm slit widths. The excitation wavelength was 284 nm, and the emission spectra were recorded from 300 to 400 nm.

Synchronous Fluorescence Spectroscopy. Synchronous fluorescence spectra of HSA in the absence and presence of

increasing amounts of phthalate plasticizers were measured under the same conditions with steady-state fluorescence.

UV-Vis Absorption Spectroscopy. UV-vis absorption spectroscopy was performed on a TU-1810 UV-vis absorption spectrophotometer (Beijing, China) equipped with 1.0 cm quartz cells. The range of wavelength was from 190 to 300 nm.

CD Spectroscopy. CD measurements were performed using an Olis DSM 1000 automatic recording spectrophotometer in a 1 mm quartz cell at room temperature. Each spectrum represented the average of five successive scans. CD spectra were recorded in the range of 200–260 nm. The α -helical content of HSA was calculated from the molar ellipticity ($[\theta]$) at 208 nm using the equation¹²

$$\alpha\text{-helix (\%)} = \left\{ \frac{(-[\theta]_{280} - 4000)}{(33\,000 - 4000)} \right\} \times 100 \quad (1)$$

FT-IR Spectroscopy. FT-IR measurements were carried out at room temperature on a Nicolet Nexus 670 FT-IR spectrometer equipped with a germanium attenuated total reflection (ATR) accessory, a DTGS KBr detector, and a KBr beam splitter. All spectra were taken via the ATR method with resolution of 4 cm^{-1} and 60 scans. Spectra processing procedures involved spectra of buffer being collected under the same conditions. Then, the absorbance of the buffer solution was subtracted from the spectra of the sample solution to obtain the FT-IR spectra of the protein. The subtraction criterion was that the original spectrum of protein solution between 2200 and 1800 cm^{-1} was featureless.¹³

Three-Dimensional Fluorescence Spectroscopy. Three-dimensional fluorescence spectra were performed under the following conditions: the emission wavelength was recorded from 220 to 500 nm, the initial excitation wavelength was set to 220 nm with increment of 5 nm, the number of scanning curves was 27, and other scanning parameters were just the same as those of the fluorescence quenching spectra.

Molecular Modeling. The binding models between phthalate plasticizers and HSA were generated by the AutoDock software package (version 4.2).¹⁴ Preparations of all ligands and the protein were performed with Auto Dock Tools (ADT). The crystal structure of HSA in complex with R-warfarin was obtained from the Protein Data Bank (PDB code 1H9Z). A docking cube with an edge of 33.75 Å (a grid spacing of 0.375 Å), which encompassed the whole subdomain IIA, was used throughout docking. On the basis of the Lamarckian genetic algorithm (LGA),¹⁴ 100 runs were performed for ligands with 150 individuals in the population; the maximum numbers of energy evaluations and generations were 2.5×10^7 and 2.7×10^4 , respectively; other parameters were set as the default.¹⁵ The resulting docking solutions were subsequently clustered with a root-mean-square deviation (rmsd) tolerance of 2.0 Å and were ranked by binding energy values.

RESULTS AND DISCUSSION

Fluorescence Spectroscopy. It is well-known that an intrinsic fluorescence investigation can evaluate the changes in the conformational structure of HSA when small molecules bind to it.¹⁶ HSA has only three intrinsic fluorophores, phenylalanine (Phe), tyrosine (Tyr), and tryptophan (Trp) residues. Because the Phe residue has a very low quantum yield and the fluorescence of Tyr residue is almost totally quenched when it is ionized or close to an amino group, a carboxyl group, or a Trp residue, the intrinsic fluorescence of HSA is mainly

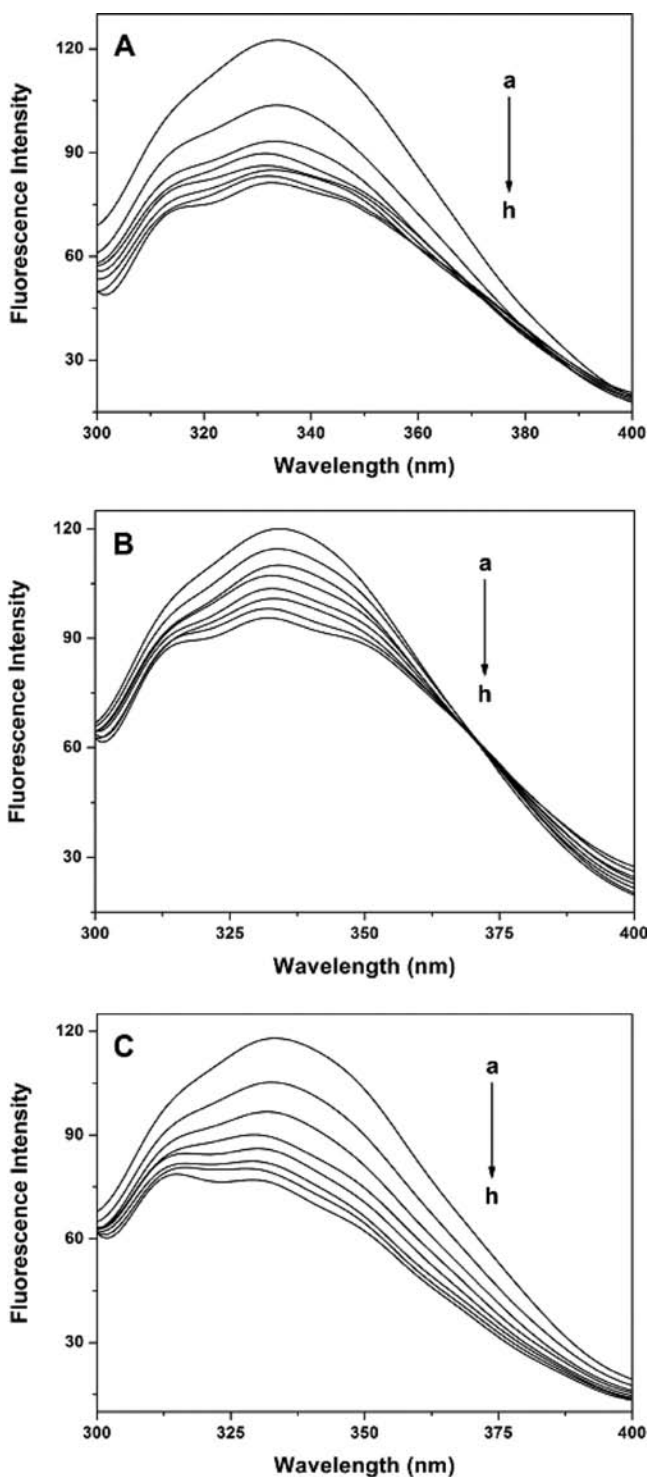


Figure 2. The fluorescence spectra of the plasticizers–HSA system. [HSA] = 3.0×10^{-6} M. (A) [DEP] = (a–h) $(1.3\text{--}8.8) \times 10^{-5}$ M; (B) [DBP] = (a–h) $(2.5\text{--}17.5) \times 10^{-6}$ M; (C) [DIBP] = (a–h) $(2.5\text{--}17.5) \times 10^{-6}$ M. $\lambda_{\text{ex}} = 284$ nm, $\lambda_{\text{em}} = 334$ nm; pH 7.4, $T = 298$ K.

contributed by the Trp residue alone.¹⁷ The fluorescence emission spectra of the plasticizers–HSA system are shown in Figure 2. It can be seen that the higher excess of phthalate plasticizers caused a gradual decrease in the fluorescence emission intensity of HSA. With the addition of phthalate plasticizers, a slightly dual fluorescence phenomena was observed for the three systems, respectively. The quenching of

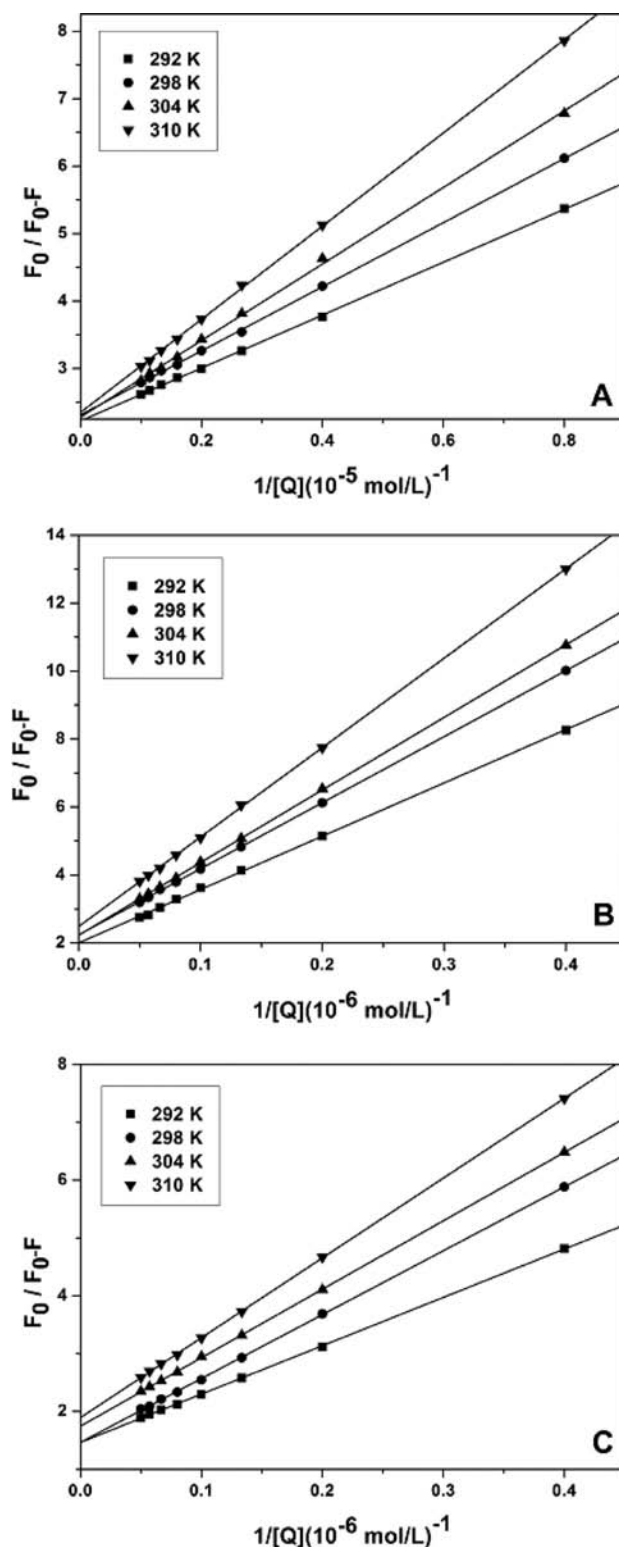


Figure 3. The modified Stern–Volmer plot of the plasticizers–HSA systems at different temperatures. [HSA] = 3.0×10^{-6} M. (A) [DEP] = $(1.3\text{--}10.0) \times 10^{-5}$ M; (B) [DBP] = $(2.5\text{--}20.0) \times 10^{-6}$ M; (C) [DIBP] = $(2.5\text{--}20.0) \times 10^{-6}$ M. $\lambda_{\text{ex}} = 284$ nm, $\lambda_{\text{em}} = 334$ nm; pH 7.4.

the fluorescence and the shift of the maximum emission wavelength of the plasticizers–HSA complex (from 334 to 332 nm for DEP, to 331 nm for DBP, and to 329 nm for DIBP) indicated that the binding of the three ligands to protein altered the microenvironment of Trp residue and the conformational

Table 1. Binding Constants for the Interaction of HSA and Plasticizers

temp (K)	binding constants K ($\times 10^5$ M $^{-1}$)		
	DEP-HSA	DBP-HSA	DIEP-HSA
292	0.57	1.28	1.75
298	0.49	1.15	1.60
304	0.40	1.04	1.47
310	0.34	0.94	1.37

structure of HSA. Simultaneously, the blue-shift in the fluorescence maximum spectra also suggested a reduction in the polarity of the microenvironment of Trp residue for the three systems.

Binding Constant and Quenching Mechanism. Data from the fluorescence experiments can be analyzed using a modified Stern–Volmer equation¹⁸

$$\frac{F_0}{F_0 - F} = \frac{1}{fK} \frac{1}{[Q]} + \frac{1}{f} \quad (2)$$

where F_0 and F are the relative fluorescence intensities of protein in the absence and presence of quencher, respectively. $[Q]$ is the quencher concentration, f is the fractional maximum fluorescence intensity of protein summed up, and K is binding constant. The plot of $F_0/(F_0 - F)$ versus $1/[Q]$ is linear with $1/fK$ as the slope and $1/f$ as the intercept. The binding constant K is a quotient of the intercept $1/f$ and slope $1/fK$.

Figure 3 is the modified Stern–Volmer plot of phthalate plasticizers with HSA at different temperatures (292, 298, 304, and 310 K) obtained from the fluorescence titration experiment, respectively. The binding constants obtained from the modified Stern–Volmer method are summarized in Table 1. It can be seen from the linearity of the modified Stern–Volmer plots in Figure 3 that three ligands bound to a single class of binding site on HSA. As shown in Table 1, the binding constants decreased with increasing temperature for three ligands, which was consistent with the static type of quenching mechanism. In this paper, the binding constants obtained from the modified Stern–Volmer equation were applied in the discussion of binding modes.

Binding Mode. There are essentially four types of noncovalent interactions that can play an important role in ligand binding to protein, such as hydrogen bond, van der Waals force, electrostatic force, and hydrophobic interaction force, etc. The thermodynamic parameters, enthalpy change (ΔH^0) and entropy change (ΔS^0), of binding reaction provide evidence for confirming binding modes.¹⁹ To obtain this information, the temperature dependence of the binding constants was studied at 292, 298, 304, and 310 K, respectively. If ΔH^0 does not vary significantly over the temperature range studied, its value and that of ΔS^0 can be determined from the Van't Hoff equation

$$\ln K = -\Delta H^0/RT + \Delta S^0/R \quad (3)$$

where K is the binding constant at the corresponding temperature, R is the gas constant, T is absolute temperature, and ΔH^0 and ΔS^0 are enthalpy change and entropy change, respectively.

According to the binding constants of the plasticizers–HSA system obtained at the four temperatures (292, 298, 304, and 310 K), the value of ΔH^0 and ΔS^0 can be obtained from the linear relationship between $\ln K$ and the reciprocal absolute

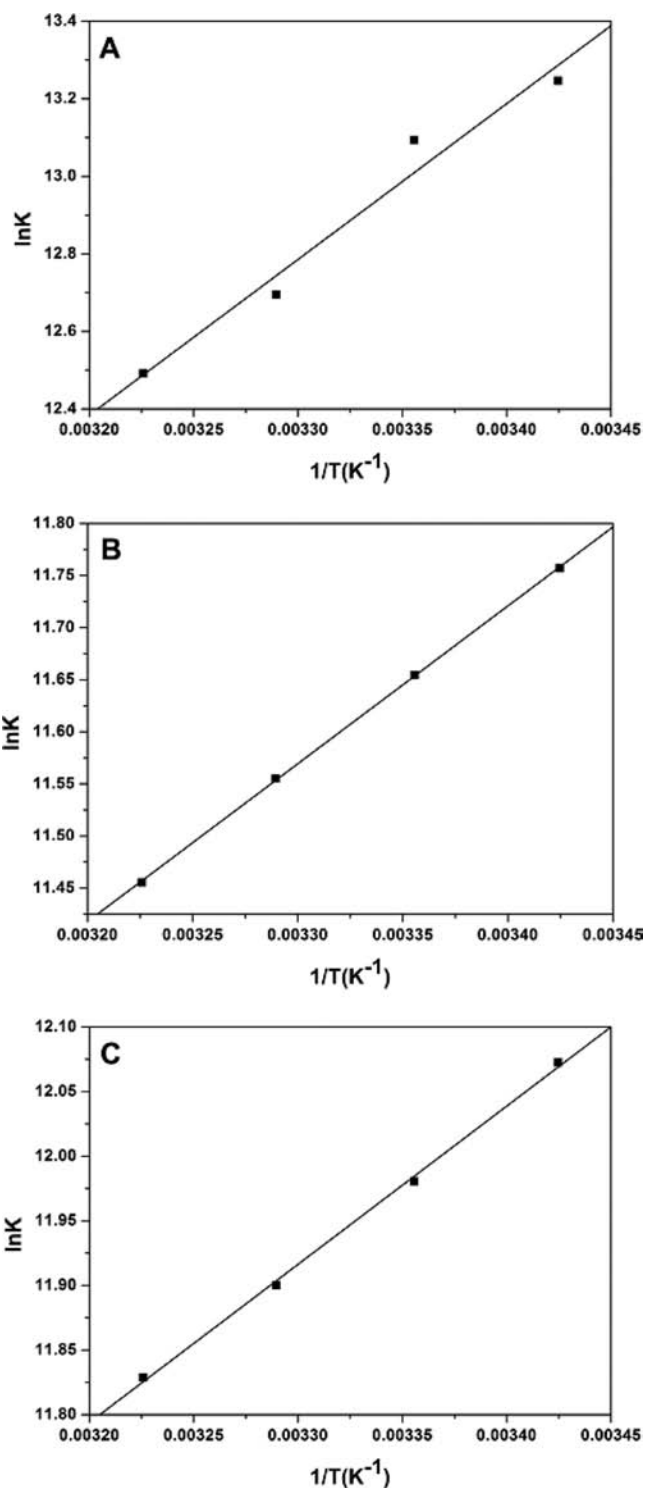


Figure 4. Van't Hoff plot of the plasticizers–HSA system in Tris buffer at pH 7.4.

temperature (Figure 4), and the free energy change (ΔG^0) can be obtained from the relationship

$$\Delta G^0 = \Delta H^0 - T\Delta S^0 \quad (4)$$

The results of the thermodynamical parameters (ΔH^0 , ΔS^0 , and ΔG^0) were listed in Table 2. From the Table, it can be seen that ΔH^0 was a small negative value, whereas ΔS^0 was a positive value for the three ligands. The negative sign for ΔG^0 indicated that the formation of the plasticizers–HSA complex was

Table 2. Thermodynamic Parameters for the Interaction of HSA and Plasticizers

temp (K)	ΔH^0 (kJ mol ⁻¹)			ΔS^0 (J mol ⁻¹ K ⁻¹)			ΔG^0 (kJ mol ⁻¹)		
	DEP	DBP	DIBP	DEP	DBP	DIBP	DEP	DBP	DIBP
292	-21.6	-12.6	-10.2	17.1	54.6	65.5	-26.6	-28.57	-29.3
298							-26.75	-28.96	-29.7
304							-26.85	-29.2	-30.1
310							-26.9	-29.55	-30.5

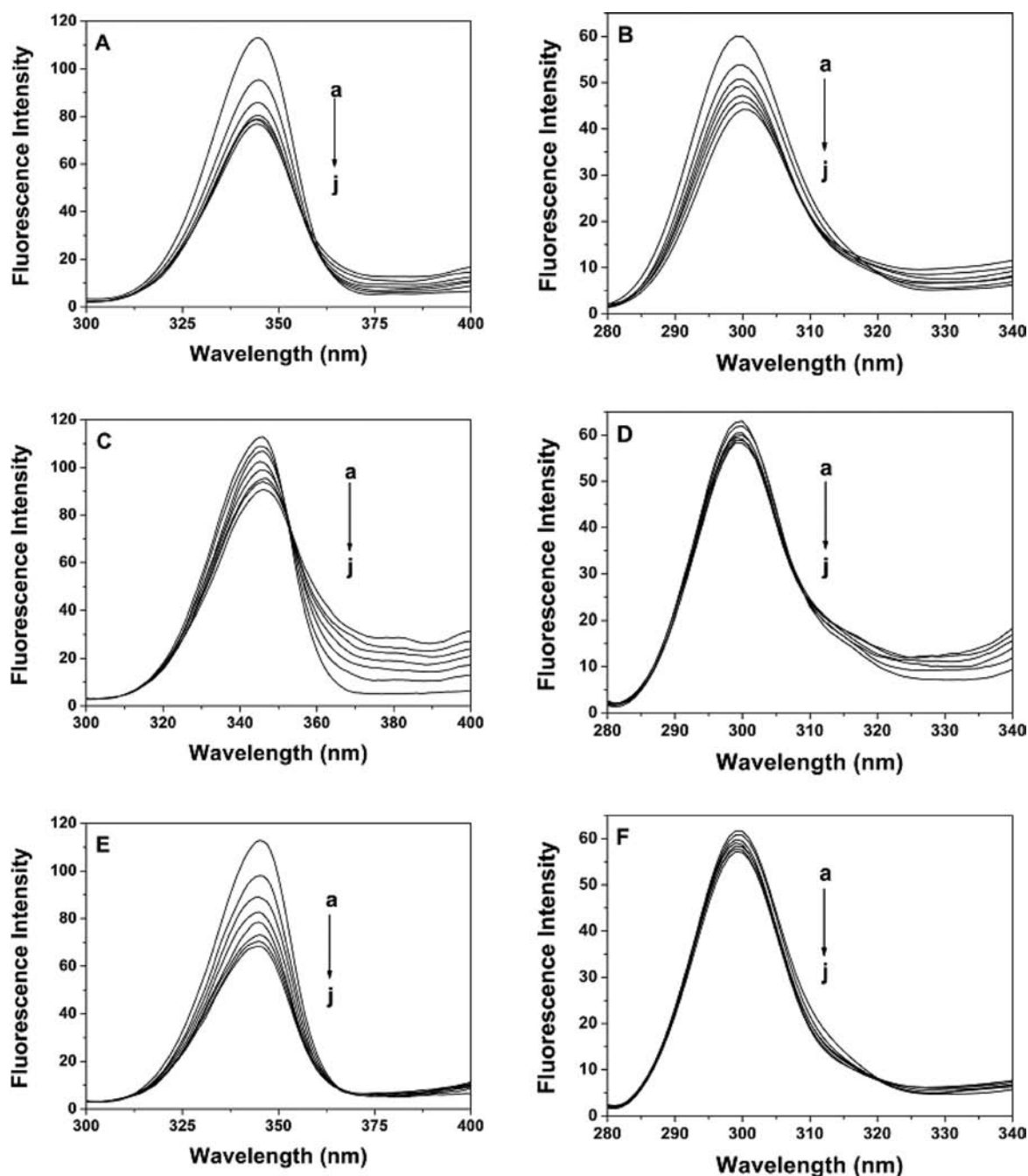


Figure 5. Synchronous fluorescence spectra of the plasticizers–HSA systems. [HSA] = 3.0×10^{-6} M. (A) [DEP] = (a–j) $(1.3\text{--}7.5) \times 10^{-5}$ M, $\Delta\lambda = 60$ nm; (B) [DEP] = (a–j) $(1.3\text{--}7.5) \times 10^{-5}$ M, $\Delta\lambda = 15$ nm; (C) [DBP] = (a–j) $(2.5\text{--}15.0) \times 10^{-6}$ M, $\Delta\lambda = 60$ nm; (D) [DBP] = (a–j) $(2.5\text{--}15.0) \times 10^{-6}$ M, $\Delta\lambda = 15$ nm; (E) [DIBP] = (a–j) $(2.5\text{--}15.0) \times 10^{-6}$ M, $\Delta\lambda = 60$ nm; (F) [DIBP] = (a–j) $(2.5\text{--}15.0) \times 10^{-6}$ M, $\Delta\lambda = 15$ nm. pH 7.4, $T = 298$ K.

entropically driven, and the binding processes were spontaneous. When molecules arranged more randomly around the three ligands and HSA resulted in the positive $\Delta S^{0,20}$ arising

from the hydrophobic contact between phthalate plasticizers and HSA. In this study, ΔH^0 was a small negative value, so the main source of the negative ΔG^0 value was derived from a

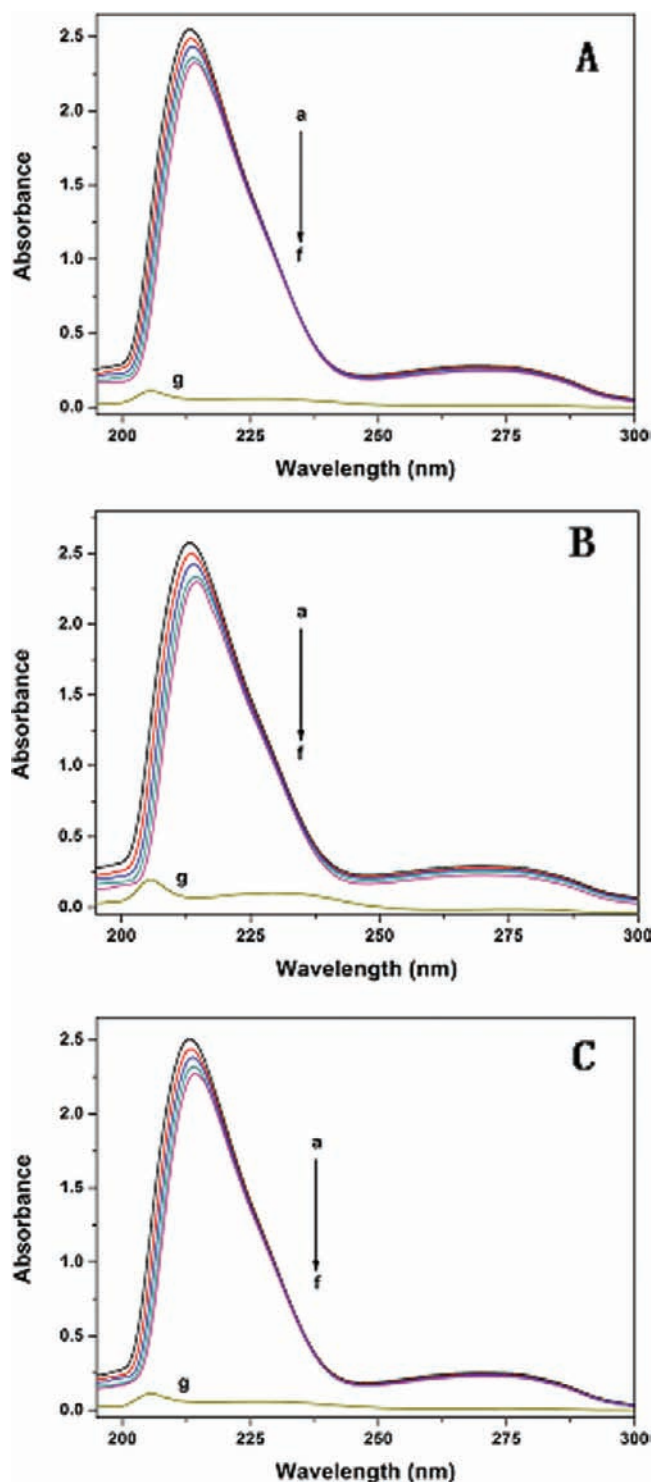


Figure 6. UV-vis absorption spectra of the plasticizers-HSA system. [HSA] = 3.0×10^{-6} M. (A) [DEP] = (a-f) $(2.5-12.5) \times 10^{-6}$ M, (g) [DEP] = 12.5×10^{-6} M; (B) [DBP] = (a-f) $(2.5-12.5) \times 10^{-6}$ M, (g) [DBP] = 12.5×10^{-6} M; (C) [DIBP] = (a-f) $(2.5-12.5) \times 10^{-6}$ M, (g) [DIBP] = 12.5×10^{-6} M. pH 7.4, $T = 298$ K.

larger contribution of a positive ΔS^0 value, indicating that the main interaction was hydrophobic contact.^{21,22} At the same time, the negative ΔH^0 value indicated there was hydrogen bonding in the interaction between phthalate plasticizers and HSA.²² Meanwhile, the above results were in good agreement with the information coming from molecular modeling.

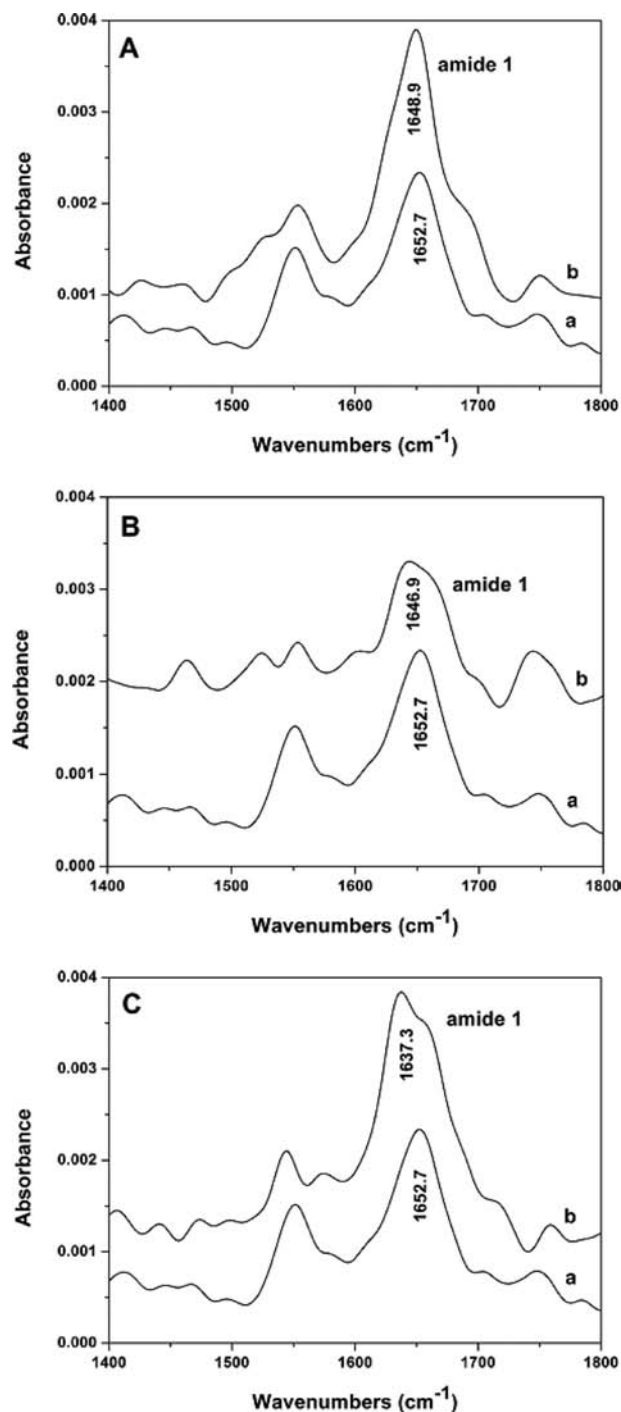


Figure 7. FT-IR spectra of free HSA (a) and difference spectra [(HSA solution + plasticizers solution) - (plasticizers solution)] (b) in Tris buffer in the region of 1800–1300 cm^{-1} . (A) (a) 3.0×10^{-5} M HSA, (b) 1.2×10^{-4} M DEP; (B) (a) 3.0×10^{-5} M HSA, (b) 1.2×10^{-4} M DBP; (C) (a) 3.0×10^{-5} M HSA, (b) 1.2×10^{-4} M DIBP. pH 7.4, $T = 298$ K.

Synchronous Fluorescence Spectra. The synchronous fluorescence spectra are frequently used to characterize the interaction between fluorescence probe and proteins because it can provide information about the molecular microenvironment in the vicinity of the chromophores molecules.²³ Generally, the fluorescence of protein comes from Trp, Tyr, and Phe residues. According to Miller,²⁴ the distinction of the difference ($\Delta\lambda$) between emission wavelength (λ_{em}) and

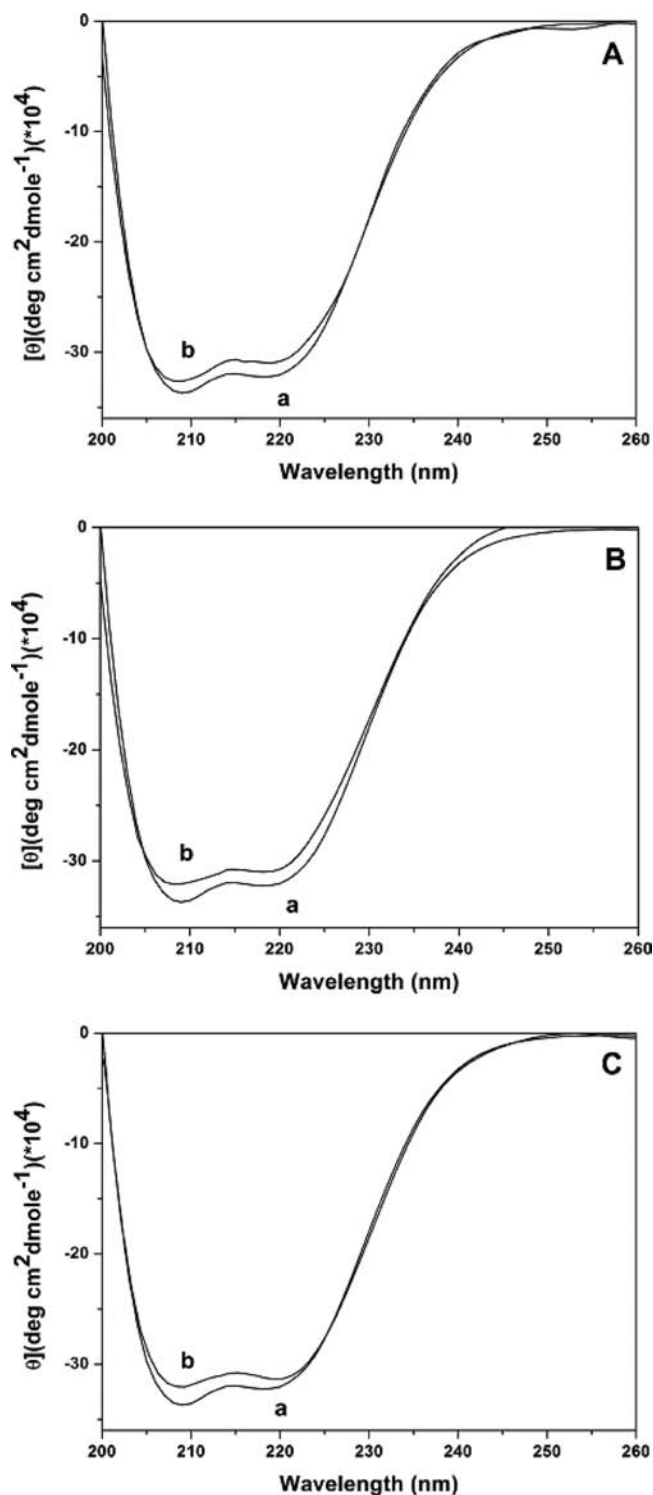


Figure 8. CD spectra of the plasticizers-HSA system. (A) (a) 3.0×10^{-6} M HSA, (b) 3.0×10^{-6} M HSA + 1.2×10^{-5} M DEP; (B) (a) 3.0×10^{-6} M HSA, (b) 3.0×10^{-6} M HSA + 1.2×10^{-5} M DBP; (C) (a) 3.0×10^{-6} M HSA, (b) 3.0×10^{-6} M HSA + 1.2×10^{-5} M DIBP. pH 7.4, $T = 298$ K.

excitation wavelength (λ_{ex}) reflects the spectra of a different nature of chromophores; when $\Delta\lambda = 60$ nm, the synchronous fluorescence spectra of HSA are characteristic of a typical Trp residue, while they are characteristic of a typical Tyr residue at a $\Delta\lambda$ value of 15 nm. Figure 5 displays the effects of addition phthalate plasticizers with varied concentrations on the

synchronous fluorescence spectrum of HSA when $\Delta\lambda$ were 60 and 15 nm. As shown in Figure 5, the fluorescence quenching of Trp and Tyr residues was observed by the addition of three ligands; nevertheless, the maximum emission wavelengths were not changed obviously when $\Delta\lambda$ were both 60 nm and 15 nm. It was indicated that the polarity around Trp and Tyr residues was changed slightly by the addition of phthalate plasticizers to HSA.

UV-Vis Absorption Spectroscopy. In order to verify the binding of phthalate plasticizers to HSA, the UV-vis absorption spectra were collected. The absorption at about 210 nm represents the α -helical structure of HSA. As shown in Figure 6, HSA has a strong absorbance with a peak at 212 nm and the absorbance was decreased with the addition of phthalate plasticizers. In addition, it can also be observed that the position of maximum absorbance peak was shifted slightly toward a longer wavelength. These two results clearly implied that an interaction occurred between phthalate plasticizers and HSA and that the conformation of HSA was changed.

FT-IR Spectroscopy. Further evidence of the conformational changes of HSA upon the addition of phthalate plasticizers was acquired by FT-IR spectroscopy. Infrared spectra of proteins exhibit a number of so-called amide bands, which represent different vibrations of the peptide moieties. Of all the amide bands of the proteins, amide I, ranging from 1600 to 1700 cm^{-1} (mainly C=O), has been widely used as a typical one,²⁵ and it has a relationship with the secondary structure of HSA. Figure 7 is the FT-IR spectra of free HSA and the difference spectra of the plasticizers-bound form of HSA. From Figure 7 it can be seen that the peak position of the amide I band shifted evidently from 1652.7 to 1648.9 cm^{-1} after addition of DEP (to 1646.9 cm^{-1} for DBP and to 1637.3 cm^{-1} for DIBP). The changes of these peak positions and peak shapes indicated that phthalate plasticizers interacted with the C=O in the protein polypeptides and caused the change of secondary structures of the HSA.

CD Spectroscopy. CD spectroscopy is a quantitative technique to investigate the secondary changes of proteins in aqueous solution. CD spectra of HSA with various concentrations of phthalate plasticizers at pH 7.40 are shown in Figure 8. It was apparently obtained that CD spectrum of free HSA exhibited characteristic features of the α -helical structure of protein with negative bands in the ultraviolet region at 208 and 222 nm in buffer solution, both due to $n \rightarrow \pi^*$ transfer for the peptide bond of α -helical.²⁰ It can be seen from Figure 8 that the binding of phthalate plasticizers to HSA decreased the band intensity at 208 and 222 nm of HSA without any significant shift of the peaks, indicating that there was a slight reduction of the α -helical content in HSA. CD spectra of HSA in presence and absence of phthalate plasticizers were similar in shape, which implied that the structure of HSA was also predominantly α -helical. The calculated results indicated a small reduction of α -helix structures from 52.0 to 49.9% at a molar ratio HSA:DEP of 1:4 and to 49.3% and to 49.1% at the same molar ratio for DBP-HSA and DIBP-HSA systems, respectively. The above results showed that the binding of phthalate plasticizers to HSA induced small conformational changes in the overall structure of HSA, which agreed with the conclusion from UV-vis and FT-IR spectroscopy.

Three-Dimensional Fluorescence Spectra. Three-dimensional fluorescence spectrum has become a powerful method for studying the interaction between a ligand with HSA in recent years. It can extensively reflect the fluorescence

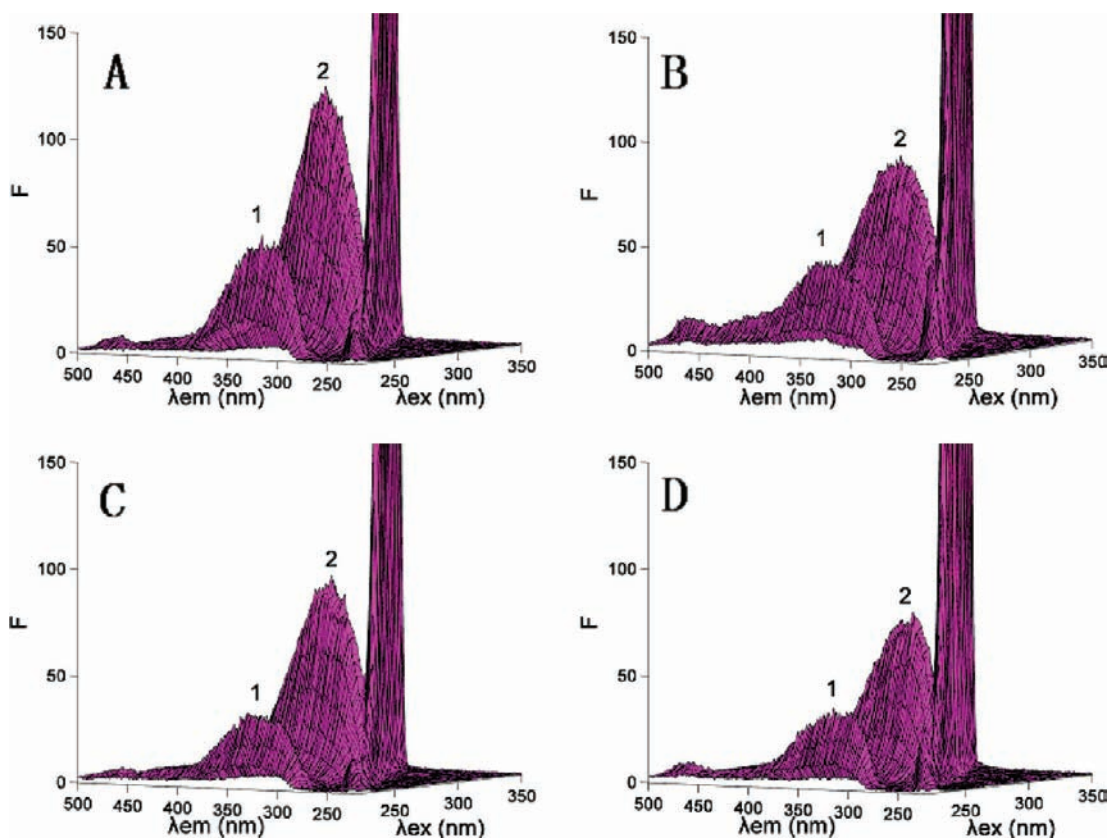


Figure 9. The three-dimensional fluorescence spectra of free HSA (A) and the plasticizers–HSA system (B, C, D). [HSA] = 3.0×10^{-6} M. [DEP] = 3.0×10^{-5} M; [DBP] = 3.0×10^{-5} M; [DIBP] = 3.0×10^{-5} M. pH 7.4, $T = 298$ K.

information of the protein, making investigation of the characteristic conformational changes of HSA more convenient and credible.²⁶ The three-dimensional fluorescence spectra of free HSA and the plasticizers–HSA system are shown in Figure 9. From Figure 9, peak 1 ($\lambda_{\text{ex}} = 280$ nm, $\lambda_{\text{em}} = 334$ nm), which mainly reveals the spectral characteristics of Trp and Tyr residues, is the primary fluorescence peak. Besides peak 1, there is another fluorescence peak, 2 ($\lambda_{\text{ex}} = 230$ nm, $\lambda_{\text{em}} = 334$ nm), that mainly exhibits the fluorescence spectral behavior of HSA's polypeptide backbone structure.²⁷ As can be seen from Figure 9, the fluorescence emission intensity of peak 1 decreased with an increasing concentration of phthalate plasticizers, implying that the microenvironment of Trp and Tyr residues was altered. Peak 2 can yield the same results, suggesting that the peptide strands structure of HSA also had been changed. The above analysis revealed that the interaction of phthalate plasticizers with HSA induced a conformational transformation in HSA.

The Energy Transfer between HSA and Phthalate Plasticizers. Energy transfer between small molecules and proteins has been widely used to study ligand–HSA interaction and change in conformation of HSA upon binding to a ligand under solution conditions.²⁸ According to the Förster non-radiative resonance energy transfer theory,²⁹ energy transfer would happen if the following conditions exist: (a) the donor can produce fluorescence, (b) the fluorescence emission spectrum of the donor and the UV–vis absorption spectrum of the acceptor overlap, and (c) the distance between the donor and the acceptor is less than 8 nm.²⁹ The distance between the donor (Trp residue) and the acceptor (plasticizers) can be calculated according to the theory. The efficiency of energy transfer (E) from donor to acceptor is related to the distance

(R_0) in this case between HSA and plasticizing agents using the equation

$$E = 1 - \frac{F}{F_0} = \frac{R_0^6}{R_0^6 + r^6} \quad (5)$$

where F_0 and F are the fluorescence intensities without and with plasticizing agents, respectively, r is the binding distance between donor and receptor, and R_0 is the Förster critical distance between donor and acceptor, at which 50% of the excitation energy is transferred to acceptor and can be obtained from donor emission and acceptor absorption spectra according to the equation

$$R_0^6 = (8.79 \times 10^{-25}) K^2 N^{-4} \Phi J \quad (6)$$

where K^2 is the orientation factor related to the geometry of the donor and acceptor of dipoles, N is the average refractive index of the medium in the wavelength range where spectral overlap is significant, Φ is the fluorescence quantum yield of the donor, and J is the overlap integral of the fluorescence emission spectrum of the donor and the absorption spectrum of the receptor, which could be calculated by the equation

$$J = \frac{\sum F(\lambda) \varepsilon(\lambda) \lambda^4 \Delta\lambda}{\sum F(\lambda) \Delta\lambda} \quad (7)$$

where $F(\lambda)$ is the fluorescence intensity of the fluorescence donor when the wavelength is λ and $\varepsilon(\lambda)$ is the molar absorbance coefficient of the acceptor at the wavelength of λ .

Figure 10 is the overlap between the fluorescence emission spectrum of HSA and the UV–vis absorption spectrum of

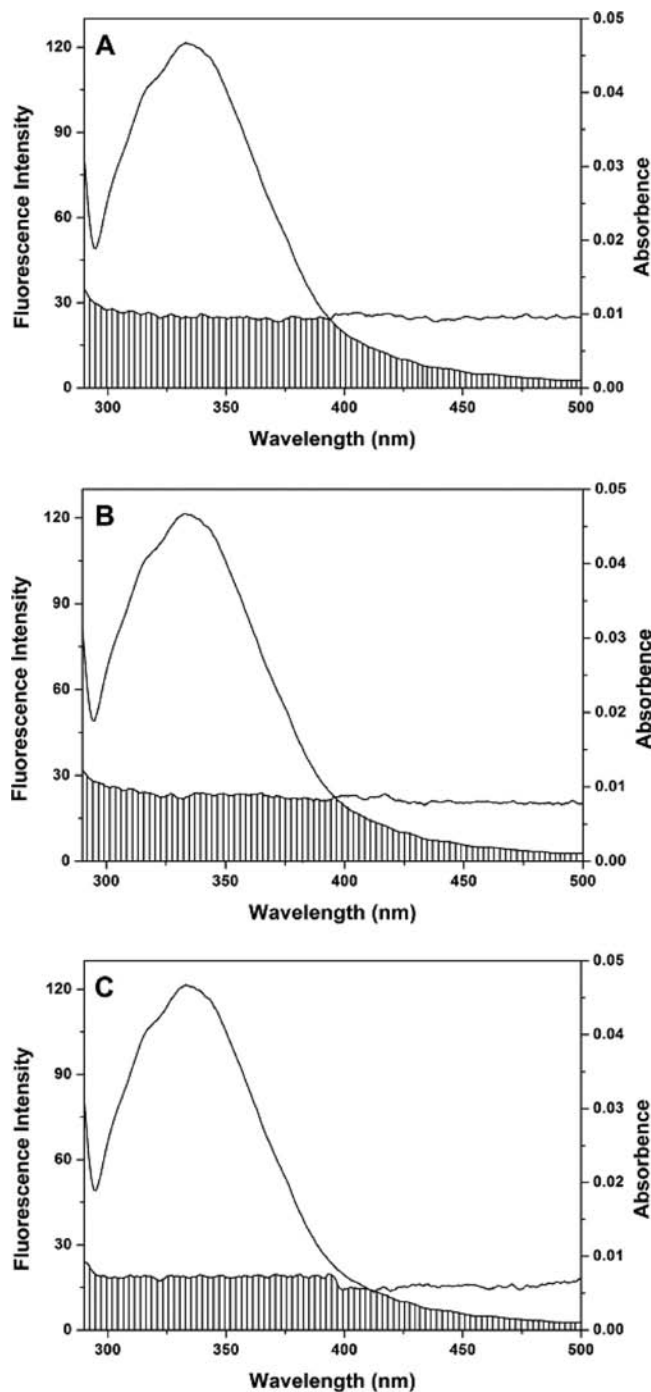


Figure 10. Overlapping between the fluorescence emission spectrum of HSA (a) and the UV-vis absorption spectrum of plasticizers (b). [HSA] = 3.0×10^{-6} M. (A) [DEP] = 3.0×10^{-6} M; (B) [DBP] = 3.0×10^{-6} M; (C) [DIBP] = 3.0×10^{-6} M. pH 7.4, $T = 298$ K.

plasticizer. In the present case, $K^2 = 2/3$, $\Phi = 0.14$, and $N = 1.36$.³⁰ According to eqs 5–7, we could calculate that $r = 3.21$ nm for DEP, $r = 2.80$ nm for DBP, and $r = 2.33$ nm for DIBP. From this data, it was suggested that the energy transfer phenomenon between HSA and the three ligands efficiently occurred.

Identification of Binding Sites on HSA. The investigation of the crystal structure analysis of HSA shows that HSA contains three structurally homologous domains, I (residues 1–195), II (residues 196–383), and III (residues 384–585), each

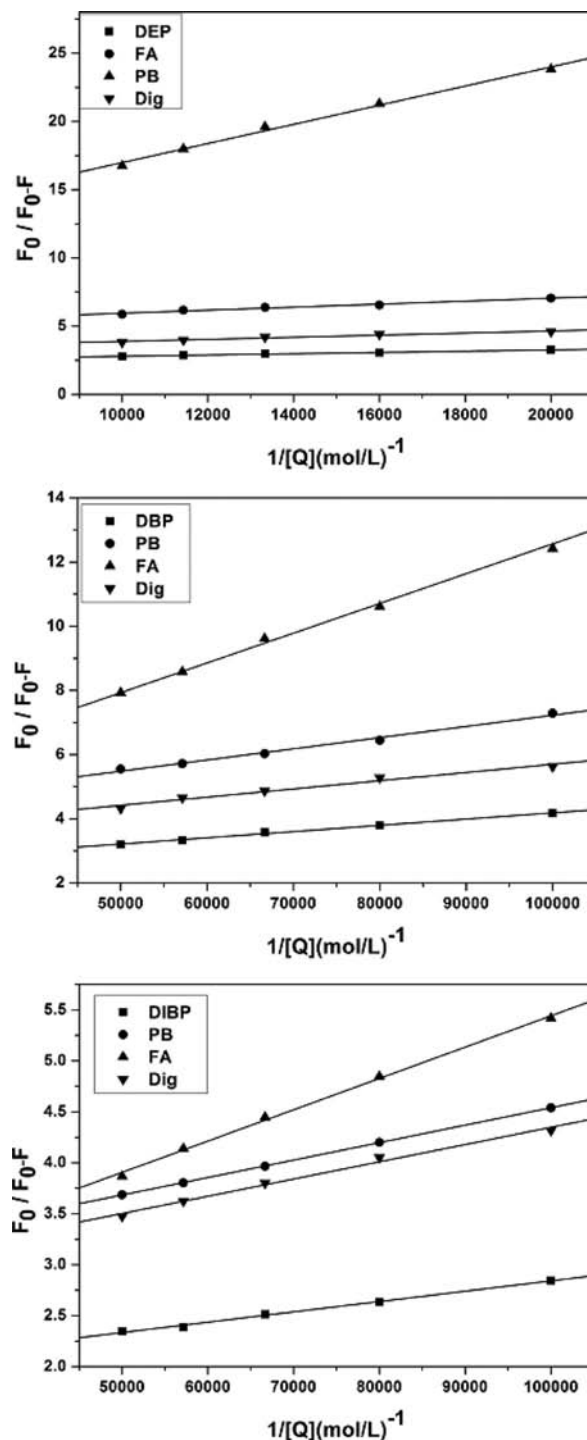


Figure 11. Effect of the site marker probe on the fluorescence of the plasticizers–HSA system. [HSA] = 3.0×10^{-6} M, [FA] = 1.0×10^{-3} M, [PB] = 1.0×10^{-3} M, [Dig] = 1.0×10^{-3} M, [DEP] = $(1.3\text{--}6.3) \times 10^{-5}$ M, [DBP] = $(2.5\text{--}12.5) \times 10^{-6}$ M, [DIBP] = $(2.5\text{--}12.5) \times 10^{-6}$ M. $\lambda_{\text{ex}} = 284$ nm, $\lambda_{\text{em}} = 334$ nm. pH 7.4.

of which can be divided into two subdomains (A and B).³¹ The principal regions of ligand binding sites of HSA are located in hydrophobic cavities in subdomains IIA and IIIA, which are consistent with sites I and II, respectively, and the only Trp residue (Trp-214) of HSA located in site I.³¹

Many ligands, such as warfarin and PB, were found to bind preferentially to site I of HSA, while ibuprofen, FA, etc. showed affinity for site II. Later studies indicated that Dig binding is

Table 3. Effect of Site Marker Probe for the Interaction of HSA and Plasticizers

binding constants	DBP–HSA	DEP–HSA	DIBP–HSA
$K (\times 10^5 \text{ M}^{-1})$	0.49	1.15	1.60
PB ($\times 10^5 \text{ M}^{-1}$)	0.14	0.39	0.77
FA ($\times 10^5 \text{ M}^{-1}$)	0.48	1.06	1.57
Dig ($\times 10^5 \text{ M}^{-1}$)	0.41	1.23	1.65

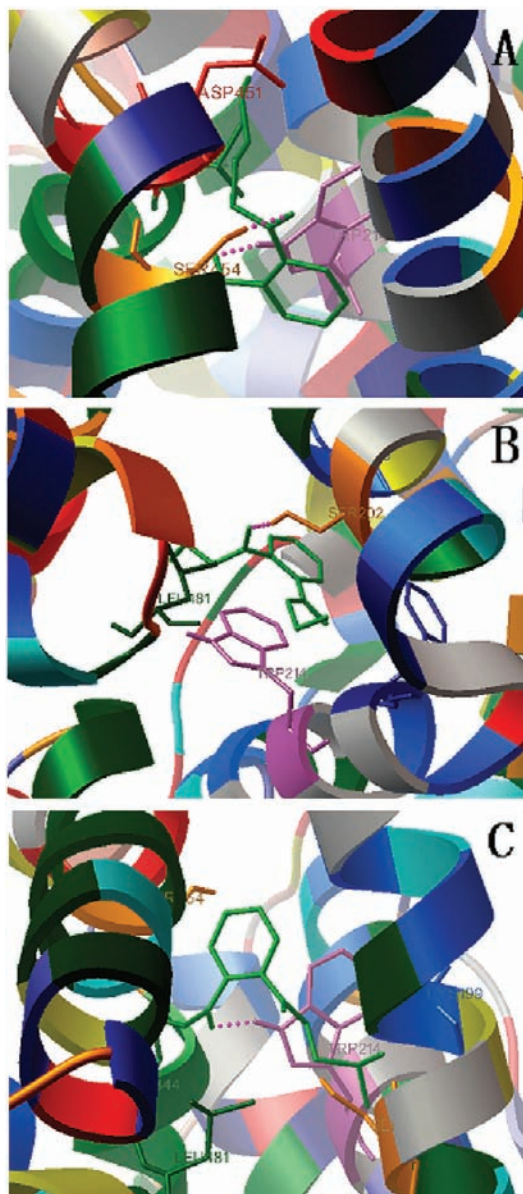


Figure 12. The best docked result of the plasticizers–HSA system: (A) DEP–HSA, (B) DBP–HSA, and (C) DIBP–HSA. The ligand structure is represented using a green stick model. The hydrogen bond between phthalate plasticizers and HSA is represented using a rose-colored dashed line.

independent of sites I and II,³² and it binds to what was nominated as site III. To further classify the binding site of HSA in which phthalate plasticizers were located, competition displacement experiments were carried out. A ternary mixture of PB, FA, or Dig and three ligands with HSA were studied, respectively. In this paper, the competitors used including PB, a characteristic marker for site I; FA for site II; and Dig for site

III. As shown in Figure 11 and Table 3, according to the modified Stern–Volmer equation, the binding constants were remarkably decreased after the addition of PB, while the addition of FA and Dig did not change the binding constants distinctly. The results calculated indicated that the interaction between phthalate plasticizers and HSA can be affected by addition of PB, that is to say, PB can displace all the three ligands from the site of HSA, but FA and Dig have no effect on the binding of them to HSA. The results probably indicated that the three ligands had one reactive site in HSA, that is, the high affinity site IIA (site I). Other significant evidence come from the results of the linear modified Stern–Volmer plots (Figure 3), which implied there was a binding site for phthalate plasticizers in proximity of Trp residue.

Molecular Modeling Study. In order to further confirm the binding site of HSA on which phthalate plasticizers were located, the complementary applications of molecule modeling also have been employed by computer methods. The best docked result between phthalate plasticizers and HSA are shown in Figure 12. The binding results indicated that three ligands molecule moiety were adjacent to the hydrophobic residues Trp-214, Ser-454, Leu-481, etc., which implied the existence of a hydrophobic interaction between phthalate plasticizers and HSA. At the same time, it is important to note that the Trp-214 residue of HSA was in close proximity to phthalate plasticizers, so all the results coming from the molecular modeling method illuminated that phthalate plasticizers could interact with HSA at site I. These conclusions provided a good structural basis to explain the efficient fluorescence quenching of HSA emission in the presence of phthalate plasticizers and well agreed with the thermodynamic analysis and the study to identify the binding sites.

On the other hand, there were hydrogen interactions between the three ligands and HSA: 1-O of DEP and residue Ser-202 of HSA; 1-O of DBP and residue Trp-214 of HSA, 1-O of DBP and residue Ser-454 of HSA; 1-O of DIBP and residue Trp-214 of HSA. Meanwhile, the calculated free energy of binding (ΔG^0) values were -21.57 , -25.37 , and -27.13 kJ mol^{-1} for DEP, DBP, and DIBP, respectively, which were very close to the experimental data.

According to this study, the three phthalate plasticizers and HSA can interact with each other in vitro under simulative physiological conditions. This new assay is helpful to understand the mechanism of the biological effects, functions, and toxicity of phthalate plasticizers in biological processes, implying the potential theoretical foundation for the study of the harm from phthalate plasticizers to the human body. Therefore, it is valuable for the food security.

ABBREVIATIONS USED

HSA, human serum albumin; DEP, diethyl phthalate; DBP, dibutyl phosphate; DIBP, diisobutyl phthalate; PB, phenylbutazone; FA, flufenamic acid; Dig, digitoxin; CD, circular dichroism; FT-IR, Fourier transform infrared; ATR, attenuated total reflection; Phe, phenylalanine; Tyr, tyrosine; Trp, tryptophan; PDB, Protein Data Bank

■ AUTHOR INFORMATION

Corresponding Author

*E-mail: chenxg@lzu.edu.cn. Fax: 86-931-8912582. Tel: 86-931-8912763.

Funding

We are grateful for financial support from the National Natural Science Foundation of China (No. 21075056, J0730425) and the Fundamental Research Funds for the Central Universities (lzujbky-2010-40).

REFERENCES

(1) Robert, B. Hazard to the developing male reproductive system from cumulative exposure to phthalate esters—Dibutyl phthalate, diisobutyl phthalate, butylbenzyl phthalate, diethylhexyl phthalate, dipentyl phthalate, and diisononyl phthalate. *Regul. Toxicol. Pharmacol.* **2009**, *53* (2), 90–101.

(2) Xie, X. Y.; Wang, Z. W.; Zhou, X. M.; Wang, X. R.; Chen, X. G. Study on the interaction of phthalate esters to human serum albumin by steady-state and time-resolved fluorescence and circular dichroism spectroscopy. *J. Hazard. Mater.* **2011**, *192* (3), 1291–1298.

(3) Staples, C. A.; Peterson, D. R.; Parkerton, T. F.; Adams, W. J. The environmental fate of phthalate esters: A literature review. *Chemosphere* **1997**, *35* (4), 667–749.

(4) Zhang, Z. B.; Hu, Y.; Zhao, L.; Li, J.; Bai, H. C.; Zhu, D. S.; Hu, J. Y. Estrogen agonist/antagonist properties of dibenzyl phthalate (DBzP) based on in vitro and in vivo assays. *Toxicol. Lett.* **2011**, *207* (1), 7–11.

(5) Boberg, J.; Metzdorff, S.; Wortziger, R.; Axelstad, M.; Brokken, L.; Vinggaard, A. M.; Dalgaard, M.; Nellemann, C. Impact of diisobutyl phthalate and other PPAR agonists on steroidogenesis and plasma insulin and leptin levels in fetal rats. *Toxicology* **2008**, *250* (2–3), 75–81.

(6) Casajuana, N.; Lacorte, S. New methodology for the determination of phthalate esters, bisphenol A, bisphenol A diglycidyl ether, and nonylphenol in commercial whole milk samples. *J. Agric. Food Chem.* **2004**, *52* (12), 3702–3707.

(7) Kuo, P. L.; Hsu, Y. L.; Huang, M. S.; Tsai, M. J.; Ko, Y. C. Ginger suppresses phthalate ester-induced airway remodeling. *J. Agric. Food Chem.* **2011**, *59* (7), 3429–3438.

(8) Carter, D. C.; Ho, J. X. Structure of serum albumin. *Adv. Protein Chem.* **1994**, *45*, 153–203.

(9) Xiao, J. B.; Chen, L. S.; Yang, F.; Liu, C. X.; Bai, Y. L. Green, yellow and red emitting CdTe QDs decreased the affinities of apigenin and luteolin for human serum albumin in vitro. *J. Hazard. Mater.* **2010**, *182* (1–3), 696–703.

(10) Matei, I.; Ionescu, S.; Hillebrand, M. Interaction of fisetin with human serum albumin by fluorescence, circular dichroism spectroscopy and DFT calculations: Binding parameters and conformational changes. *J. Luminesc.* **2011**, *131* (8), 1629–1635.

(11) Zhang, Z. H.; Xu, D. P.; Tie, M.; Li, F. Y.; Chen, Z. L.; Wang, J.; Gao, W.; Ji, X. T.; Xu, Y. Spectroscopic study on interaction between bisphenol A or its degraded solution under microwave irradiation in the presence of activated carbon and human serum albumin. *J. Luminesc.* **2011**, *131* (7), 1386–1392.

(12) Khan, M. A.; Muzammil, S. Musarrat, Differential binding of tetracyclines with serum albumin and induced structural alterations in drug-bound protein. *Int. J. Biol. Macromol.* **2002**, *30* (5), 243–249.

(13) Dong, A. C.; Huang, P.; Caughey, W. S. Protein secondary structures in water from second-derivative amide I infrared spectra. *Biochemistry* **1990**, *29* (13), 3303–3308.

(14) Morris, G. M.; Goodsell, D. S.; Halliday, R. S.; Huey, R.; Hart, W. E.; Belew, R. K.; Olson, A. J. Automated docking using a Lamarckian genetic algorithm and an empirical binding free energy function. *J. Comput. Chem.* **1998**, *19* (14), 1639–1662.

(15) Lu, S. Y.; Jiang, Y. J.; Lv, J.; Wu, T. X.; Yu, Q. S.; Zhu, W. L. Molecular docking and molecular dynamics simulation studies of GPR40 receptor–agonist interactions. *J. Mol. Graph. Model.* **2010**, *28* (8), 766–774.

(16) Yang, X. Z.; Wu, D. C.; Du, Z. L.; Li, R. X.; Chen, X. L.; Li, X. H. Spectroscopy study on the interaction of quercetin with collagen. *J. Agric. Food Chem.* **2009**, *57* (9), 3431–3435.

(17) Sulkowska, A. Interaction of drugs with bovine and human serum albumin. *J. Mol. Struct.* **2002**, *614* (1–3), 227–232.

(18) Lakowicz, J. R. *Principles of Fluorescence Spectroscopy*; Plenum Press: New York, 1983; pp 258–265.

(19) Mallick, A.; Haldar, B.; Chattopadhyay, N. Spectroscopic investigation on the interaction of ICT probe 3-Acetyl-4-oxo-6,7-dihydro-12H indolo-[2,3-a] quinolizine with serum albumins. *J. Phys. Chem. B* **2005**, *109* (30), 14683–14690.

(20) Yue, Y. Y.; Zhang, Y. H.; Zhou, L.; Qin, J.; Chen, X. G. In vitro study on the binding of herbicide glyphosate to human serum albumin by optical spectroscopy and molecular modeling. *J. Photochem. Photobiol. B—Biol.* **2008**, *90* (1), 26–32.

(21) Rahman, M. H.; Maruyama, T.; Okada, T.; Yamasaki, K.; Otagiri, M. Study of interaction of carprofen and its enantiomers with human serum albumin—I. Mechanism of binding studied by dialysis and spectroscopic methods. *Biochem. Pharmacol.* **1993**, *46* (10), 1721–1731.

(22) Ross, P. D.; Subramanian, S. Thermodynamics of protein association reactions: Forces contributing to stability. *Biochemistry* **1981**, *20* (11), 3096–3102.

(23) Gong, A. Q.; Zhu, X. S.; Hu, Y. Y.; Yu, S. H. A fluorescence spectroscopic study of the interaction between epristeride and bovine serum albumin and its analytical application. *Talanta* **2007**, *73* (4), 668–673.

(24) Miller, J. N. Recent advances in molecular luminescence analysis. *Proc. Anal. Div. Chem. Soc.* **1979**, *16*, 203–208.

(25) Sirotkin, V. A.; Zinatullin, A. N.; Solomonov, B. N.; Faizullin, D. A.; Fedotov, V. D. Calorimetric and Fourier transform infrared spectroscopic study of solid proteins immersed in low water organic solvents. *Biochim. Biophys. Acta* **2001**, *1547* (2), 359–369.

(26) Zhang, Y. Z.; Chen, X. X.; Dai, J.; Zhang, X. P.; Liu, Y. X.; Liu, Y. Spectroscopic studies on the interaction of lanthanum(III) 2-oxo-propionic acid salicyloyl hydrazone complex with bovine serum albumin. *Luminescence* **2008**, *23* (3), 150–156.

(27) Wang, Y. Q.; Tang, B. P.; Zhang, H. M.; Zhou, Q. H.; Zhang, G. C. Studies on the interaction between imidacloprid and human serum albumin: Spectroscopic approach. *J. Photochem. Photobiol. B—Biol.* **2009**, *94* (3), 183–190.

(28) Hu, Y. J.; Liu, Y.; Wang, J. B. Study of the interaction between monoammonium glycyrrhizinate and bovine serum albumin. *J. Pharm. Biomed. Anal.* **2004**, *36* (4), 915–919.

(29) Sklar, L. A.; Hudson, B. S.; Simoni, R. D. Conjugated polyene fatty acids as fluorescent probes: Binding to bovine serum albumin. *Biochemistry* **1977**, *16* (23), 5100–5108.

(30) Epps, D. E.; Raub, T. J.; Caiola, V.; Chiari, A.; Zamai, M. Determination of the affinity of drugs toward serum albumin by measurement of the quenching of the intrinsic tryptophan fluorescence of the protein. *J. Pharm. Pharmacol.* **1999**, *51* (1), 41–48.

(31) He, X. M.; Carter, D. C. Atomic structure and chemistry of human serum albumin. *Nature* **1992**, *358*, 209–215.

(32) Sjöholm, I.; Ekman, B.; Kober, A.; Ljungstedt-Pahlman, I.; Seiving, B.; Sjödin, T. Binding of drugs to human serum albumin: XI. The specificity of three binding sites as studied with albumin immobilized in microparticles. *Mol. Pharmacol.* **1979**, *16* (3), 767–777.